

The effect of sheet thickness on the magnetic properties of 77 wt % Ni permalloys

T. AKOMOLAFE*, G. W. JOHNSON,

Department of Metallurgy, The University of Leeds, Leeds, LS2 9JT, UK

The effect of sheet thickness, t , on the magnetic properties of some Ni-Fe alloys of approximate composition 77% Ni-14% Fe-5% Cu-4 wt % Mo for various heat treatments in the temperature range 300 to 1250° C has been investigated. The range of sheet thickness used was 50 to 375 μm and was obtained by cold-rolling without interstage annealing. It was found that permeability increases with decreasing sheet thickness, attains a maximum at $t \simeq 75 \mu\text{m}$ and starts to fall as the thickness is further reduced. The increase in permeability with decreasing sheet thickness ($t > 75 \mu\text{m}$) is thought to be due to a decrease in eddy current losses, changes in texture formation and possibly the degree of short range order (SRO) developed in the material. The permeability obeys a $1/t^2$ relationship with sheet thickness in the range 75 to 375 μm . Below a sheet thickness of 75 μm permeability starts to decrease with decreasing sheet thickness. The reason for this fall in permeability is thought to be due to a thickness dependent magnetostatic energy contribution to the wall energy associated with free poles along the domain wall and also to the loss ratio, η , which increases rapidly at small thicknesses. This rapid increase in η is due to factors such as the ratio of domain wall spacing to sheet thickness, which varies with sheet thickness, the spin relaxation term, which has a $1/t^2$ dependence on sheet thickness, and the increase in the wall energy which increases the domain wall spacing. Finally a decrease in permeability could be caused by a different degree of SRO in the thinner specimens due to different cooling rates which could lead to an increase in first anisotropy constant, K_1 and saturation magnetostriction, λ_s which then produces a decrease in μ_i at $t < 75 \mu\text{m}$ when the degree of SRO in the specimens is not optimum.

1. Introduction

The Ni-Fe alloys in the region extending from 35-90% Ni "the permalloy" region, are extensively used in the electrical industry because of their good magnetic properties. Of interest in this region are the alloys of approximate composition 77% Ni-14% Fe-5% Cu-4 wt % Mo which possess very high relative initial permeability ($> 10^5$), low coercive force ($\cong 0.13-0.03 \text{ A m}^{-1}$), low hysteresis loss, etc, when subjected to a suitable heat treatment [1-6].

It is known that the magnetic properties of these alloys depend on the values of the anisotropy and magnetostriction constants. Both the magnitude and sign of the isotropic magnetostriction constant and of the anisotropy constant depend on the degree of SRO developed in the material. Optimum magnetic properties are obtained when a critical degree of SRO is developed in these alloys which allow both the anisotropy energy and magnetostriction constant to be simultaneously reduced to small values. The initial permeability, μ_i is known to be much more affected by anisotropy than the magnetostriction. Various degrees of order can be obtained by controlled cooling of the specimens at different rates in the temperature range between about 500 and 400° C. It is thus possible to have in turn, in the same specimens, a first

anisotropy constant, K_1 which is either

(a) negative - i.e. when the specimen is cooled at an extremely slow rate, at about 4°C h^{-1} giving $K_1 = -300 \text{ mJ m}^{-2}$;

(b) vanishingly small when the specimen is cooled at a rate of about 65°C h^{-1} or

(c) positive, when the material is cooled at a rapid rate i.e. a quench at about $10^5^\circ \text{C h}^{-1}$, giving $K_1 = 250 \text{ mJ m}^{-2}$ - [7]. Different degrees of order, giving different permeabilities, may also develop in specimens of the same composition but of different thicknesses when they are cooled at the same rate.

The most important sources of strains in those alloys, which can have marked effect on the initial permeability, is the presence of impurities held in substitutional or interstitial solution in the metal or alloy. These impurities are usually removed by heat treating the specimens at high temperature in a purified dry hydrogen atmosphere. The advantage of the initial high temperature anneal is to produce purification, strain relief (including recovery and recrystallization, grain growth, texture formation, etc. The beneficial effect of the hydrogen anneal developed [8, 9] for the purification of magnetic materials have been used to great effect [3, 5, 10, 11].

The work reported in this paper is the study of the

* Permanent address: Physics Department, University of Ilorin, Ilorin, Nigeria.

influence of sheet thickness on the magnetic properties, grain growth, texture formation and atomic ordering, of some Ni-Fe alloys of approximate composition 77% Ni-14% Fe-5% Cu-4 wt % Mo and it forms a part of a more general investigation of the magnetic properties, microstructure and magnetic domain structure of 77% Ni permalloys [12, 13].

2. Materials and experimental technique

The alloys used throughout the entire project were commercial alloys of approximate composition 77% Ni-14% Fe-5% Cu-4 wt % Mo supplied in the form of 375 μm cold-rolled sheets. As commercial alloys, they contain varying amounts of added and impurity elements such as manganese, tungsten, cobalt, carbon, chromium, sulphur, silicon, phosphorus and aluminium. It was not known to what extent these existed as oxides, carbides and nitrides, nor was it known how they were dispersed through the material. Silicon, magnesium and manganese are added as deoxidants, however, aluminum and manganese in addition, are also used as desulphurizers and for improving hot workability respectively [12]. Required thicknesses were obtained by cold-rolling the materials without interstage annealing.

To achieve the best magnetic properties such as high permeabilities, low hysteresis loss and low coercivity, the materials were given an initial high temperature anneal at 1100°C for 4 h in a purified dry hydrogen atmosphere with a dew point of about -60°C. During this heat treatment, processes such as purification, strain-relief (including recovery and recrystallization) and texture formation occur in the materials.

Initial permeability measurements were made on specimens in the form of annular rings of 17.5 mm inside diameter and 25.4 mm outside diameter, punched from the sheet material. For the permeability measurements the standard method, in which the specimens were used as the core of an inductor, was used. The permeability of the specimens was then calculated from the measured inductance of the toroid. The standard toroid was formed of five heat-treated rings stacked loosely, with paper laminations, in plastic formers around which ten turns of PVC covered copper wire were wound. The inductance of the toroid was measured using a Wayne Kerr Universal Bridge and a null detector tuned to the internal frequency of the oscillator of the Wayne Bridge at 1592 Hz. Permeability measurements were made on materials of different thicknesses which had undergone various heat treatments. The effects of sheet thickness on atomic ordering, recrystallization and grain growth, and texture were also studied.

3. Results and discussion

Microstructural changes and permeability measurements were made on quenched and furnace-cooled specimens of various thicknesses ranging between 50 and 375 μm . It should be pointed out at this stage that we are only interested in the shapes of the curves obtained in the results discussed here rather than the absolute values of μ_i remembering the fact that

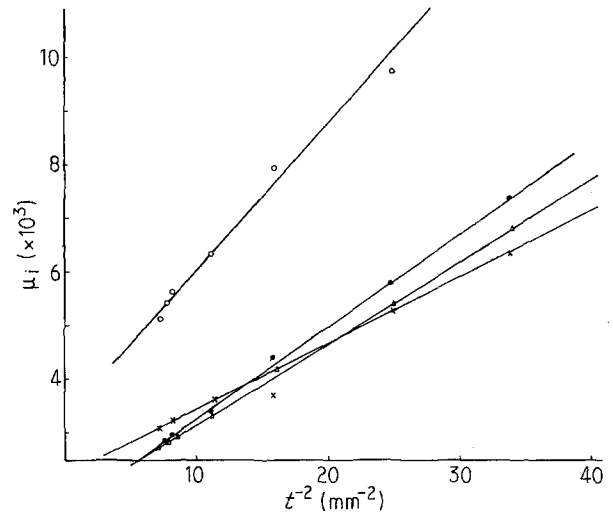


Figure 1 Effect of sheet thickness, t on permeability, μ_i for furnace-cooled and quenched (O 1100°C 4 h)-(● from 1100°C, Δ from 600°C, × from 1250°C) specimens.

permeability measurements were made at a frequency of 1592 Hz.

The effect of sheet thickness t on the initial permeability, μ_i was investigated. The specimen thicknesses used were in the range between 50 and 375 μm . For the range of sheet thickness used, it was found that permeability increases with decreasing sheet thickness, though not linearly. In order to establish the relationship between the sheet thickness and the initial permeability it was decided to plot a graph of μ_i against $1/t^2$ from the obtained data. Fig. 1 shows the graph of μ_i plotted against $1/t^2$ for different heat treatments. All the graphs are linear which shows that μ_i obeys a $1/t^2$ relationship, i.e.

$$\mu_i = Ct^{-2} \quad (1)$$

where C , the constant of proportionality is given by [5]

$$C = \frac{3\rho}{2\pi^2 Qf\eta} \quad (2)$$

where ρ is the resistivity of the material measured with direct current, f the measuring frequency, η the loss ratio and Q the ratio of the reactive and resistive components introduced by the core material. Using Equations 2 and 1 it can be seen that the improvement in permeability due to the reduction of sheet thickness is due to a decrease in eddy current losses, changes in texture formation and possibly the degree of SRO developed in the material. The higher permeabilities of furnace-cooled material is due to the production of a significant degree of SRO during the slow cool through the ordering temperature range.

In Fig. 2 it can be seen that the permeability increases with decreasing sheet thickness. Initially, the permeability increases with annealing time, attains a maximum, then decreases and levels off as the annealing time is increased.

It should be pointed out at this stage that prior to the ordering anneals the materials were given high temperature anneals at 1100°C for 4 h and furnace cooled. During the cooling in the ordering temperature range different degrees of SRO developed in each material. Consequently, this could be the reason why

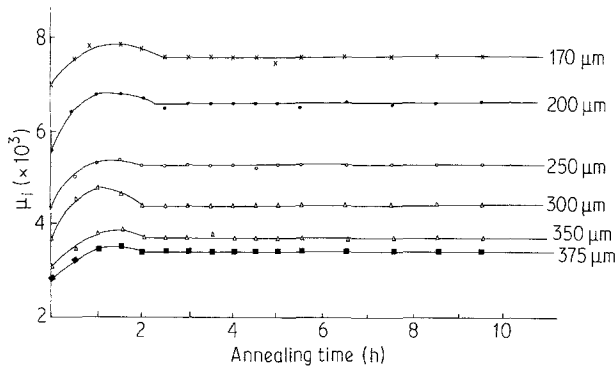


Figure 2 Graph of initial permeability, μ_i plotted against ordering time t for various sheet thicknesses (Note ordering temperature – 420°C.)

the different thicknesses have different μ_i at zero time. During the ordering anneals, the increase in permeability is due to an increase in the degree of SRO. At an optimum degree of SRO the permeability is a maximum and when the optimum degree of SRO is exceeded the permeability falls. The SRO attains an equilibrium value with increase in annealing time and the graphs level off.

Fig. 3 shows the results obtained when the materials were annealed at 600°C and quenched. The graphs are horizontal because a negligible amount of SRO is produced. Again from these graphs it could be seen that permeability increases with decreasing sheet thickness.

In order to establish separately the influence of grain size and texture formation on the permeability with decreasing thickness, investigations were carried out to monitor the effect of sheet thickness on the grain size and texture formation.

When $t < 75 \mu\text{m}$ the permeability falls. One of the factors which could account for the observed decrease in permeability with decreasing sheet thickness is the thickness-dependent magnetostatic contribution to the wall energy associated with the free poles along the domain wall. The permeability is proportional to an inverse power of the wall energy γ [7]. The wall surface energy γ of a Bloch wall is given by [15]:

$$\gamma = \pi^2 \frac{A}{a} + \frac{aK}{2} + \pi a^2 I_s^2 / (a + t) \quad (3)$$

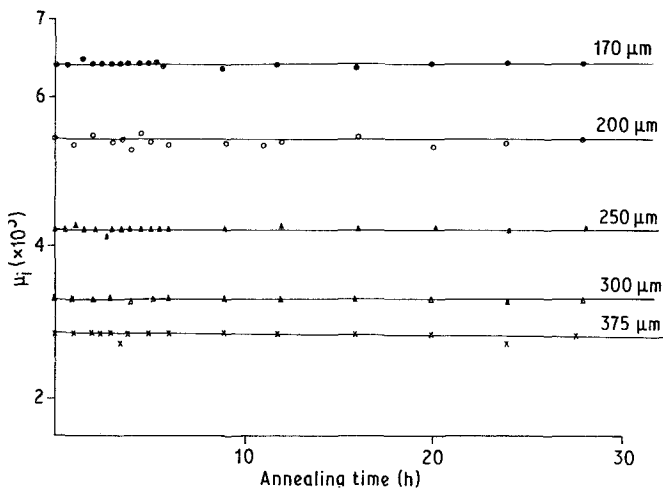


Figure 3 Graph of initial permeability μ_i plotted against ordering time t for various sheet thicknesses. (Note ordering temperature – 600°C.)

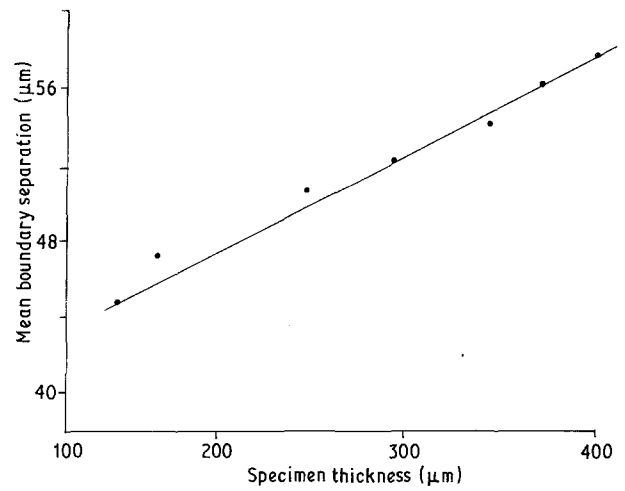


Figure 4 Graph of mean boundary separation, d plotted against sheet thickness.

where A is the exchange energy constant, a the width of the domain wall, K a uniaxial anisotropy constant, and t the sheet thickness.

From Equation 3 it is seen that as the sheet thickness decreases the third term on the right-hand side (the magnetostatic term) increases, causing an increase in γ . Because of the inverse power proportionality between permeability and the wall energy, permeability falls with decreasing sheet thickness. Hence, using Equation 3 it can be seen that the decrease in permeability for $t < 75 \mu\text{m}$ is consistent with mathematical prediction [15] and experimental works [5, 7] where a fall in permeabilities of their sheet material when the thickness was less than 80 and 100 μm respectively, was observed. It was argued that the permeability of thinner specimens appears to be determined not only by the dominant anisotropy energy but also by a thickness dependent magnetostatic contribution to the wall energy.

Fig. 4 shows the effect of sheet thickness on mean boundary separation, d . From these results it can be seen that the mean boundary spacing decreases with decreasing sheet thickness. In sheet material the grains cease growing soon after they extend across the sheet thickness. The reason for this is that the effectively two-dimensional grain boundary tension equilibrium involved is more easily reached than a three-dimensional one in which the only known equilibrium arrangement is that of identical Kelvin tetrakaidecahedra. Also the reduction of mean boundary spacing with decreasing sheet thickness is due to the pinning effects of grooves formed where the grain boundaries emerge at the specimen surface. The grooves may be formed by cold-work or thermal etching. Fig. 5 shows the effect of grain size, or mean grain boundary separation, on permeability. The result shows that the permeability appears to decrease with increase in grain size. Generally the influence of grain size on the initial permeability will depend on the method used to produce the different grain sizes in the material. If different grain sizes are obtained by a method of isothermal annealing at a temperature greater than the recrystallization temperature where texture formation, changes in the degree of SRO, eddy current losses (material of the same thickness) magneto-

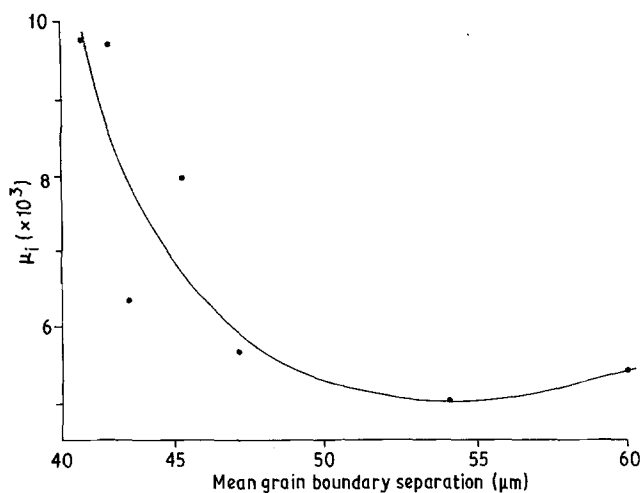


Figure 5 Graph of initial permeability μ_i plotted against mean grain boundary separation.

striction and anisotropy constants are kept constant, then the permeability increases linearly with increasing grain size [12] and has a relationship of the form:

$$\mu_i = ad + b \quad (4)$$

where a is a grain size factor, d the grain size diameter, and b a constant which depends on impurity content. Hence it could be concluded at this stage that the increase in permeability with decreasing grain size could be due to the degree of SRO, decrease in eddy current losses and possibly texture formation in the material (to be discussed later).

The effect of sheet thickness on cold-rolled and recrystallization texture, were investigated. In the case of the cold-rolled specimens, the intensity of deformation texture components such as $\{110\} \langle 111 \rangle$ and $\{112\} \langle 111 \rangle$ increased with deformation [13]. The reason for this being that as the degree of deformation increases more grains are being given favourable rotations towards the $\{110\} \langle 111 \rangle$ and $\{112\} \langle 111 \rangle$ directions; possibly because the increase in stored energy limits the number of slip systems in operation. These results are consistent with the observations of [14] on some fcc metals and alloys. From these results it could be inferred that the per-malloy has a low stacking fault energy.

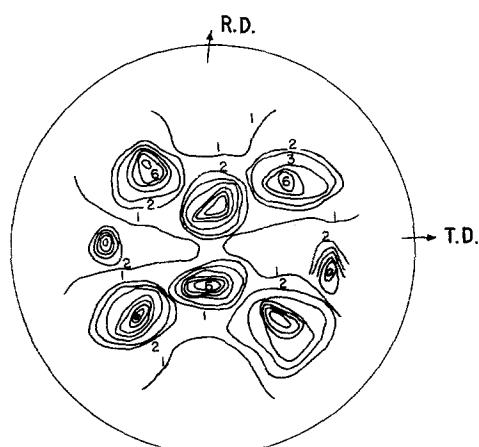


Figure 6 $\{111\}$ pole figure showing a strongly developed cube texture $\{100\} \langle 001 \rangle$ and $\{146\} \langle 211 \rangle$ and $\{123\} \langle 412 \rangle$ deformation textures for a specimen of $375 \mu\text{m}$ thickness. T.D., Transverse Direction; R.D., Rolling Direction.

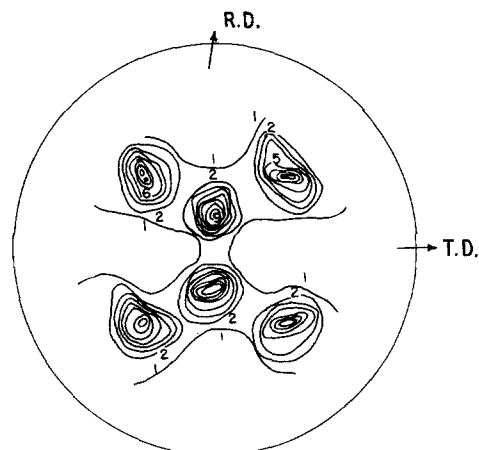


Figure 7 $\{111\}$ pole figure showing a more strongly developed optimum cube texture $\{100\} \langle 001 \rangle$ and a weaker deformation texture due to an optimum annealing of 4 h at 1100°C (Note Specimen = $250 \mu\text{m}$ thick). T.D., Transverse Direction; R.D., Rolling Direction.

Figs 6 and 7 show the $\{111\}$ pole figures for two thicknesses 375 and $250 \mu\text{m}$ respectively annealed at 1100°C for 4 h. From Fig. (7) it could be seen that the cube texture $\{100\} \langle 001 \rangle$ increased as the degree of deformation increases. The increase in the intensity of the cube texture is known to increase the initial permeability. Secondly, the intensity of the deformation texture components retained after annealing decreases with cold-work, i.e. as the sheet thickness decreases. The deformation textures $\{146\} \langle 211 \rangle$ and $\{123\} \langle 412 \rangle$ seen in Fig. 6 for the $375 \mu\text{m}$ thick material were highly reduced in Fig. 7. The reduction and absence of some of the deformation textures due to additional cold-rolling could be because the nuclei for these components might have been sufficiently rotated away from these directions, or the nuclei might be too small and their growth rate could be very small compared with crystals of other orientations. From these results it can be concluded that reduction of sheet thickness leads to an increase in the intensity of the cube texture $\{100\} \langle 001 \rangle$ which should invariably lead to an improvement in the initial permeability of the materials with decreasing sheet thickness.

In order to be able to study the influence of eddy current losses on the permeability the specimens were further cold-rolled down to $50 \mu\text{m}$. Fig. 8 (plotted from Table I) shows the effect of sheet thickness on the

TABLE I Effect of sheet thickness on permeability

Sheet thickness (μm)	μ_i furnace cooled	μ_i quenched at 600°C
50	25 490	7251
60	26 748	8260
75	27 515	8985
80	27 520	9445
90	22 253	8746
140	13 745	6756
170	9751	7008
200	9745	5748
250	7995	4506
300	5253	3748
350	5492	3070
360	5230	3009
375	5004	2507

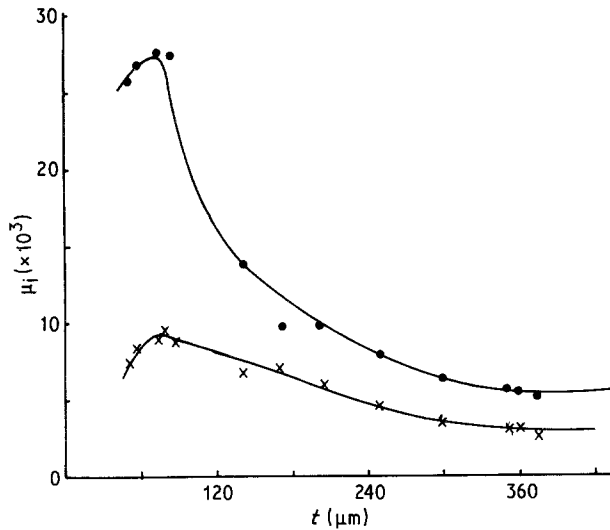


Figure 8 Variation of the initial permeability, μ_i with sheet thickness for different heat treatments (● annealed 4 h at 1100°C, × quenched at 600°C).

initial permeability for a thickness range of 50 to 375 μm for the furnace cooled and quenched specimens. Between 375 and 75 μm permeability increases with decreasing sheet thickness and reaches a maximum at about 75 μm and starts to fall when the sheet thickness, t is further reduced. For a sheet thickness which lies between 75 and 375 μm (i.e. for $t > 75 \mu\text{m}$) permeability obeys Relation 1 i.e. $\mu_i = Ct^{-2}$ and this result is consistent with the results obtained in Fig. 1.

Another factor which could account for the decrease in permeability as the sheet thickness, t , is decreased ($t < 75 \mu\text{m}$) is the loss ratio η , i.e. C in Equation 2 will no longer be a constant but vary with the sheet thickness. The loss ratio, η , defined as the ratio of observed to calculated eddy current loss, increases rapidly with decreasing sheet thickness at small thicknesses.

The effect of sheet thickness on the loss ratio, η [5] is shown in Fig. 10. Various workers have explained this variation as being due to the presence of surface layers whose permeability is less than that of the bulk material. These are known to arise quite naturally from surface closure-domains or could be due to impurities existing only on the surface. Further the loss ratio, η , is known to depend on the ratio of

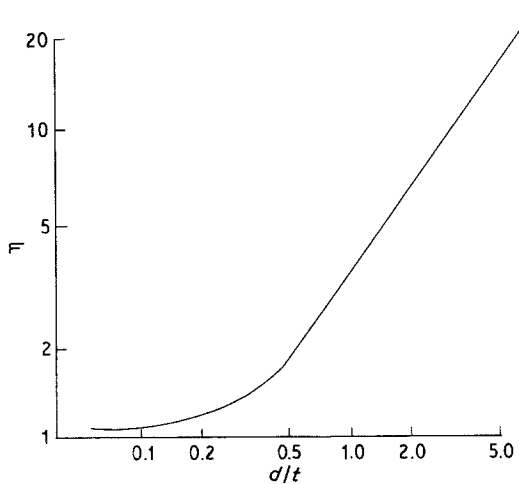


Figure 9 Variation of loss ratio, η with d/t .

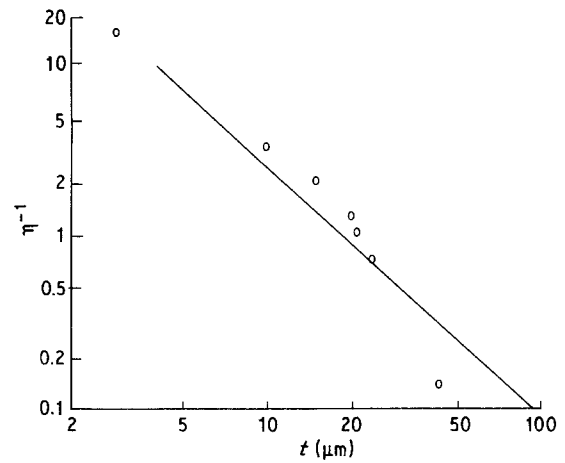


Figure 10 Variation of loss ratio η as a function of sheet thickness.

domain wall spacing d to sheet thickness, t . The relationship between η and the ratio d/t in the absence of spin relaxation effect, is of the form [16]:

$$\eta = \frac{96}{\pi^3} \cdot \frac{d}{3} \sum' n^{-3} \coth \frac{n\pi d}{3} \quad (5)$$

where the summation is over odd values of n . Fig. 9 shows a plot of Equation 5. For the values of $d/t < 1$, Equation 5 becomes fairly well approximated by an expression of form:

$$\eta = 1 + at^{-r}. \quad (6)$$

Fig. 10 shows the effect of sheet thickness, t , on the loss ratio, η [5]. From this graph, [5] discovered that $a = 90$ and $r = 3/2$ if the thickness, t is in micrometres.

The value of $r = 3/2$ [5] is in fair agreement with the prediction of Lee [16] that r lies between 1.5 and 1.7. If the sheet thickness is decreased to a few micrometres such that d is also decreased, then the spin relaxation term takes control of η and $r = 2$, (i.e. $\eta \propto t^{-2}$), this assumption is based on d being constant which is not true. It was indicated [16] that since the anomalous eddy current loss is not a function of frequency (for $f < 100 \text{ kHz}$) then the loss ratio, η , is due to a relaxation mechanism.

A further factor which will influence the loss ratio is the wall energy, γ . An increase in the wall energy of Equation 3 would also lead to an increase in the domain wall spacing which then leads to a decrease in permeability.

A decrease in permeability with decreasing sheet thickness could also be due to changes in the degree of SRO in the thinner materials ($t < 75 \mu\text{m}$) due to different rates of cooling. The change could produce an increase in both the magnetostriction and anisotropy constants. This interpretation is in accordance with the findings of Jackson [17] with work on 76% Ni, 77% Ni and 78% Ni permalloys. Jackson [17] indicated that there was an increase in magnetostriction with decreasing sheet thickness, and magnitude of the increase depends on the nickel content of the alloy, being substantial in the 76% and 77% Ni. It was also indicated by Kittel [18] that there is a close physical relationship which exists between the anisotropy and magnetostriction constants (though the precise nature

is not known in ferromagnetics). He showed that magnetostriction gives rise to an apparent contribution to anisotropy energy of the crystal. Hence it is plausible at this stage to expect that there would be variations in K_1 and λ_s due to sheet thickness.

Finally, a decrease in permeabilities in the thinner specimens could occur due to variations in the mobilities of 180° walls under a.c. conditions due to interactions between the domain walls and surface irregularities or because of modifications to the domain wall structure near the surface. Eddy current and hysteresis losses in the thinner material would be affected by changes in wall mobilities. These effects have been noted to cause an increase in η in 50/50 and 65/35 Ni-Fe alloys; and a consequent decrease in μ_i .

4. Conclusion

It was noted that permeability increases with decreasing sheet thickness, attains a maximum at $t \simeq 75 \mu\text{m}$ and starts falling as t is further reduced. The improvement in permeability with decreasing sheet thickness obeys a t^{-2} law and this is thought to be due to increase in the intensity of cube texture $\{100\} \langle 001 \rangle$ formation, reduction in eddy current losses and possibly the degree of SRO which favours the reduction of K_1 and λ_s to be simultaneously reduced to small values. The maximum permeability at $t \simeq 75 \mu\text{m}$ could correspond to a state when the grain size, texture formation, eddy current losses have optimum value. The decrease in permeability at $t < 75 \mu\text{m}$ could be due to the rapid increase in η with decreasing sheet thickness, since η depends on such factors as the ratio of domain wall spacing d to sheet thickness, t , spin relaxation term, wall energy, γ , and domain wall

mobilities. Finally, variations in the degree of SRO in the thinner specimens due to different cooling rates could lead to increase in K_1 and λ_s which leads to a decrease in μ_i at $t < 75 \mu\text{m}$.

References

1. G. W. ELMEN, *J. Frank. Inst.* **206** (1928) 317.
2. T. D. YENSEN, *ibid.* **145** (1923) 621.
3. R. M. BOZORTH, "Ferromagnetism", (Van Nostrand, New York, 1951).
4. *Idem*, *Rev. Mod. Phys.* **25** (1953) 42.
5. C. E. RICHARDS, A. C. LYNCH and E. V. WALKER, *Proc. I.E.E. B* **104** (1957) 343.
6. R. D. ENOCH and A. D. FUDGE, *Brit. J. Appl. Phys.* **17** (1966) 623.
7. R. D. ENOCH and A. WINTERBORN, *I.E.E. Conf. Publ.* **33** (1967) 123.
8. P. P. CIOFFI, *Phys. Rev.* **39** (1934) 742.
9. T. D. YENSEN and N. A. ZEIGLER, *Trans. Ame Soc. Met.* **24** (1936) 337.
10. D. L. BOOTHBY and R. M. BOZORTH, *J. Appl. Phys.* **18** (1947) 173.
11. D. A. COLLING and R. G. ASPDEN, *ibid.* **41** (1969) 1571.
12. T. AKOMOLAFE, PhD Thesis, University of Leeds (1983).
13. T. AKOMOLAFE and G. W. JOHNSON, *J. Mater. Sci.* **22** (1987) 95.
14. I. L. DILLAMORE and W. T. ROBERTS, *Acta Metall.* **12** (1964) 281.
15. S. MIDDELHOEK, *J. Appl. Phys.* **34** (1963) 1054.
16. E. W. LEE, *I.E.E. Mon* **284M** (1958).
17. R. C. JACKSON, PhD Thesis, Nottingham University (1958).
18. C. KITTEL, *Rev. Mod. Phys.* **21** (1949) 555.

Received 23 June 1987

and accepted 2 June 1988